Preprints

2nd IFAC Workshop on Fractional Differentiation and its Applications

19 - 21 July, 2006
Porto, Portugal

IFAC

isep
Instituto superior de engenharia do porto

INSTITUTO POLITÉCNICO DO PORTO

FCT

Proceedings of the 2nd IFAC
Workshop on Fractional Differentiation and its Applications
Porto, Portugal, July 19-21, 2006

FRACTIONAL-ORDER HARMONICS IN THE TRAJECTORY CONTROL OF REDUNDANT MANIPULATORS

Fernando B. M. Duarte,[1] Maria da Graça Marcos,[2] J. A. Tenreiro Machado[3]

[1]*Escola Superior de Tecnologia Viseu, Dep. Matemática, Campus Politécnico, 3510 Viseu, Portugal, fduarte@mat.estv.ipv.pt.*
[2]*Instituto Politécnico do Porto, Instituto Superior de Engenharia, Dep. Matemática, Rua António Bernardino de Almeida, 4200 Porto, Portugal, mgm@isep.ipp.pt.*
[3]*Instituto Politécnico do Porto, Instituto Superior de Engenharia, Dep. Engenharia Electrotécnica, Rua António Bernardino de Almeida, 4200 Porto, Portugal, jtm@.isep.ipp.pt.*

Abstract: Redundant manipulators are superior to classical arms because they allow the trajectory optimization, the obstacle avoidance, and the resolution of singularities. For this type of manipulators, the kinematic control algorithms adopt generalized inverse matrices that may lead to unpredictable responses. Motivated by these problems this paper studies the complexity revealed by the trajectory planning scheme when controlling redundant manipulators. The result reveals a chaotic phenomenon and the existence of fractional order sub-harmonics in the robot signals. *Copyright © 2006 IFAC*

Keywords: Redundant Manipulators, Kinematics, Fractional-Order Harmonics, Fourier Transform, Windowed Fourier Transform.

1. INTRODUCTION

A kinematically redundant manipulator is a robotic arm possessing more degrees of freedom (*dof*) than those required to establish an arbitrary position and orientation of the gripper. Redundant manipulators offer several potential advantages over non-redundant arms. In a workspace with obstacles, the extra degrees of freedom can be used to move around or between obstacles and thereby to manipulate in situations that otherwise would be inaccessible (Klein, *et al.*, 1983; Yoshikawa, 1988).
When a manipulator is redundant, it is anticipated that the inverse kinematics admits an infinite number of solutions. This implies that, for a given location of the manipulator's gripper, it is possible to induce a self-motion of the structure without changing the location of the end effecter. Therefore, the arm can be reconfigured to find better postures for an assigned set of task requirements.
Several kinematic techniques for redundant manipulators control the gripper through the rates at which the joints are driven, using the pseudoinverse of the Jacobian (Klein, *et al.*, 1983). Nevertheless, these algorithms lead to a kind of chaotic motion with unpredictable arm configurations.
Having these ideas in mind, the paper is organized as follows. Section 2 introduces the fundamental issues for the kinematics of redundant manipulators. Based on these concepts, section 3 presents the trajectory control of the 3*R*-robot. The results reveal a chaotic behavior that is further analyzed in section 4. Finally, section 5 draws the main conclusions.

2. KINEMATICS OF REDUNDANT MANIPULATORS

A kinematically redundant manipulator is a robotic arm possessing more *dof* than those required to establish an arbitrary position and orientation of the gripper.

When a manipulator is redundant it is anticipated that the inverse kinematics admits an infinite number of solutions. This implies that, for a given location of the manipulator's gripper, it is possible to induce a self-motion of the structure without changing the location

of the gripper. Therefore, redundant manipulators can be reconfigured to find better postures for an assigned set of task requirements but, on the other hand, have a more complex structure requiring adequate control algorithms.

We consider a manipulator with n degrees of freedom whose joint variables are denoted by $\mathbf{q} = [q_1, q_2, ..., q_n]^T$. We assume that a class of tasks we are interested in can be described by m variables, $\mathbf{x} = [x_1, x_2, ..., x_m]^T$ ($m < n$) and that the relation between $\mathbf{q}$ and $\mathbf{x}$ is given by:

$$\mathbf{x} = f(\mathbf{q}) \tag{1}$$

where f is a function representing the direct kinematics. Differentiating (1) with respect to time yields:

$$\dot{\mathbf{x}} = \mathbf{J}(\mathbf{q})\,\dot{\mathbf{q}} \tag{2}$$

where $\dot{\mathbf{x}} \in \Re^m$, $\dot{\mathbf{q}} \in \Re^n$ and $\mathbf{J}(\mathbf{q}) = \partial f(\mathbf{q})/\partial \mathbf{q} \in \Re^{m \times n}$. Hence, it is possible to calculate a path $\mathbf{q}(t)$ in terms of a prescribed trajectory $\mathbf{x}(t)$ in the operational space. We assume that the following condition is satisfied:

$$\max \text{ rank } \{\mathbf{J}(\mathbf{q})\} = m \tag{3}$$

Failing to satisfy this condition usually means that the selection of manipulation variables is redundant and the number of these variables m can be reduced. When condition (3) is satisfied, we say that the degree of redundancy of the manipulator is $n-m$. If, for some $\mathbf{q}$

$$\text{rank } \{\mathbf{J}(\mathbf{q})\} < m \tag{4}$$

then the manipulator is in a singular state. This state is not desirable because, in this region of the trajectory, the manipulating ability is very limited. Based on these concepts, in order to analyze and quantify the problem of object manipulation, it was proposed in (Yoshikawa, 1988) the expression $\mu = [det(\mathbf{J}\mathbf{J}^T)]^{1/2}$ as a measure of the manipulability.

Most of the approaches for solving redundancy that have been proposed (Doty, *et al.*, 1993) are based on the inversion of equation (2). A solution in terms of the joint velocities is sought as:

$$\dot{\mathbf{q}} = \mathbf{J}^{\#}(\mathbf{q})\,\dot{\mathbf{x}} \tag{5}$$

where $\mathbf{J}^{\#}$ is one of the generalized inverses of the $\mathbf{J}$ (Doty, *et al.*, 1993; Siciliano, 1990).

It can be easily shown that a more general solution to equation (2) is given by:

$$\dot{\mathbf{q}} = \mathbf{J}^{+}(\mathbf{q})\,\dot{\mathbf{x}} + \left[\mathbf{I} - \mathbf{J}^{+}(\mathbf{q})\,\mathbf{J}(\mathbf{q})\right]\dot{\mathbf{q}}_0 \tag{6}$$

where $\mathbf{I}$ is the $n \times n$ identity matrix and $\dot{\mathbf{q}}_0 \in \Re^n$ is a $m \times 1$ arbitrary joint velocity vector and $\mathbf{J}^+$ is the pseudoinverse of the $\mathbf{J}$. The solution (6) is composed of two terms. The first term is relative to minimum norm joint velocities. The second term, the *homogeneous solution*, attempts to satisfy the additional constraints specified by $\dot{\mathbf{q}}_0$. Moreover, the matrix $\mathbf{I} - \mathbf{J}^+(\mathbf{q})\mathbf{J}(\mathbf{q})$ allows the projection of $\dot{\mathbf{q}}_0$ in the null space of $\mathbf{J}$. A direct consequence is that it is possible to generate internal motions that reconfigure the manipulator structure without changing the gripper position and orientation (Nakamura, 1991; Doty, *et al.*, 1993; Siciliano, 1990). Another aspect revealed by the solution of (5) is that repetitive trajectories in the operational space do not lead to periodic trajectories in the joint space. This is an obstacle for the solution of many tasks because the resultant robot configurations have similarities with those of a chaotic system.

3. ROBOT TRAJECTORY CONTROL

The direct kinematics and the Jacobian of a 3-link planar manipulator has a simple recursive nature according with the expressions:

$$\begin{bmatrix} x \\ y \end{bmatrix} = \begin{bmatrix} l_1 C_1 + l_2 C_{12} + l_3 C_{123} \\ l_1 S_1 + l_2 S_{12} + l_3 S_{123} \end{bmatrix} \tag{7.a}$$

$$\mathbf{J} = \begin{bmatrix} -l_1 S_1 - \ldots - l_2 S_{12} - \ldots - l_3 S_{123} & \ldots & l_3 S_{123} & \ldots & l_3 S_{123} \\ l_1 C_1 + \ldots + l_2 C_{12} + \ldots + l_3 C_{123} & \ldots & l_3 C_{123} & \ldots & l_3 C_{123} \end{bmatrix} \tag{7.b}$$

where l_i is the length of link i, $q_{i...k} = q_i + ... + q_k$, $S_{i...k} = Sin(q_{i...k})$ and $C_{i...k} = Cos(q_{i...k})$.

During all the experiments it is considered $\Delta t = 10^{-3}$ sec, $L_{TOT} = l_1 + l_2 + l_3 = 3$, $l_1 = l_2 = l_3$.

In the closed-loop pseudoinverse's method the joint positions can be computed through the time integration of the velocities according with the block diagram of the inverse kinematics algorithm depicted in Figure 1.

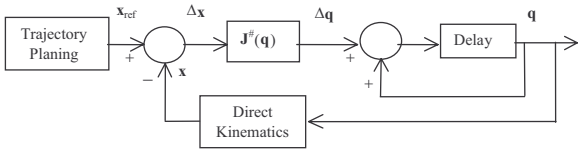

Fig. 1: Block diagram of the closed-loop inverse kinematics algorithm with the pseudoinverse.

Based on equation (7) we analyze the kinematic performances of the 3*R*-robot when repeating a circular motion in the operational space with frequency $\omega_0 = 7.0$ rad sec^{-1}, centre at $r = [x^2+y^2]^{1/2}$ and radius ρ.

Figure 2 show the joint positions and the manipulability μ for the inverse kinematic algorithm (5) for $\rho = 0.5$, when $r = \{0.6, 2.0\}$, respectively.

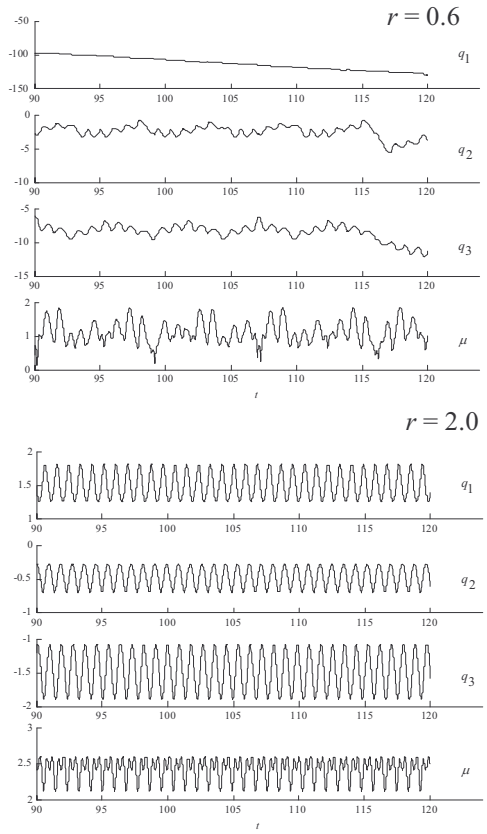

Fig. 2: The 3*R*-robot joint positions and manipulability *versus* time using the pseudoinverse method for $\rho = 0.5$ and $r = \{0.6, 2.0\}$.

We observe that:
- For r = 0.6 occur unpredictable motions with severe variations that lead to high joint transients (Duarte and Machado, 2002). Moreover, we verify a low frequency signal modulation that depends on the circle being executed. The different fractional order harmonics (*foh*) are visible in the time response but, in order to capture each *foh*, it is required to adopt a specific time window.
- For r = 2.0 the motion is periodic with frequency identical to $\omega_0 = 7.0$ rad $\sec^{-1}$.

In what concerns the index of manipulability we conclude that, for r = 0.6 it is, during some instants, very close to $\mu = 0$, while for r = 2.0 is always $\mu > 2$.

4. ANALYZING THE CHAOTIC-LIKE RESPONSES OF THE PSEUDOINVERSE ALGORITHM

In the previous section we verified that the pseudoinverse based algorithm leads to unpredictable arm configurations. Bearing these facts in mind, we analyze more deeply the robot joint signals.

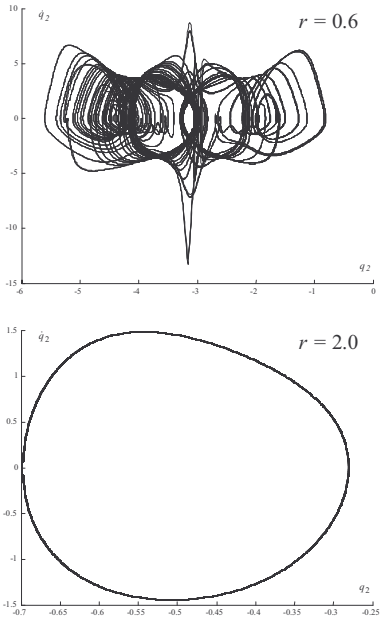

Fig. 3: Phase plane trajectory for the 3*R*-robot joint 2 during 300 cycles for $\rho = 0.5$ and $r = \{0.6, 2.0\}$.

Figure 3 depicts the phase-plane of the joint 2 trajectories when repeating a circular motion in the operational space with frequency $\omega_0 = 7.0$ rad $\sec^{-1}$, for and $\rho = 0.5$ and $r = \{0.6, 2.0\}$.

From the figures we verify that:
- For r = 0.6, besides the position and velocity drifts, leading to different trajectory loops, we have points that are 'avoided'. Such points correspond to arm configurations where several links are aligned;
- For r = 2.0 the trajectories are repetitive.

In order to gain further insight into the pseudoinverse nature several distinct experiments are devised in the sequel during a time window of 300 cycles. Therefore, in a first set of experiments we calculate the Fourier transform $F\{\ \}$ of the 3*R*-robot joints velocities for a circular repetitive motion with frequency $\omega_0 = 7.0$ rad $\sec^{-1}$, radius $\rho = \{0.5, 0.7\}$ and radial distances $r \in]0, L_{TOT} - \rho[$.

Figures 4-5 show $|F\{\dot{q}_2(t)\}|$ *versus* ω_0/ω and r.

Induced by the gripper repetitive motion ω_0 an interesting phenomenon is verified, because a large part of the energy is distributed along several sub-harmonics. These *foh* depend on r and ρ making a complex pattern with similarities with those revealed by chaotic systems. Furthermore, we observe the existence of several distinct regions depending on r.

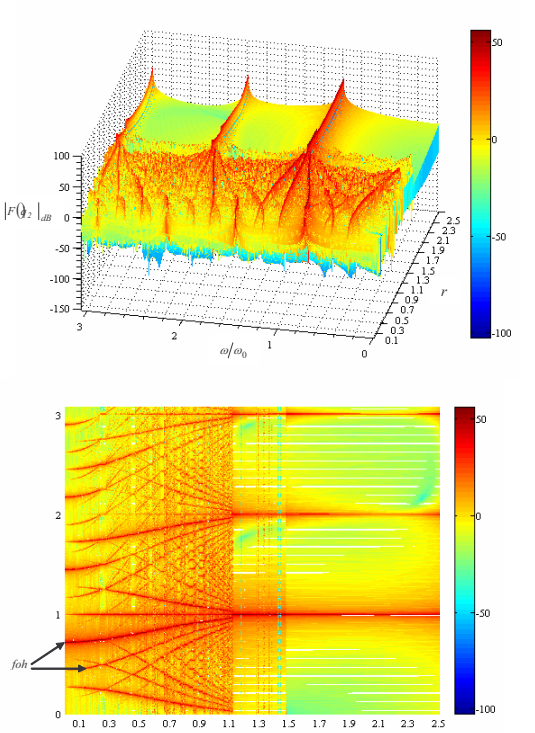

Fig. 4: $\left|F\{\dot{q}_2(t)\}\right|$ of the 3*R*-robot during 300 cycles, vs r and frequency ratio ω/ω_0, for $\rho = 0.5$, $\omega_0 = 7.0$ rad sec^{-1}.

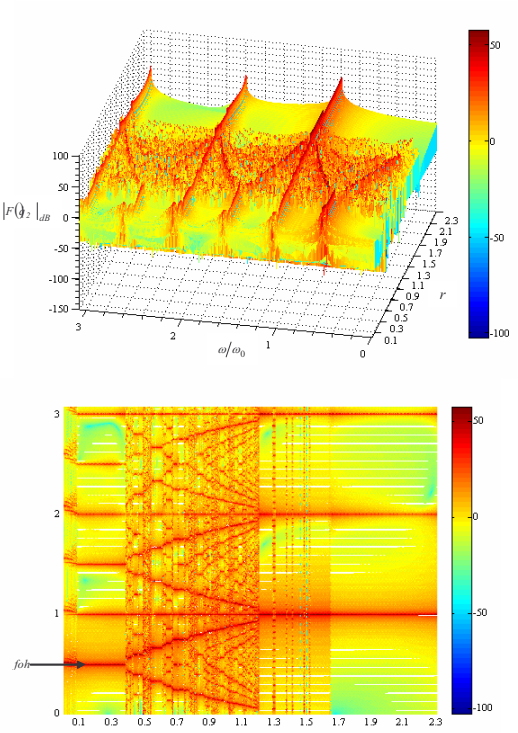

Fig. 5: $\left|F\{\dot{q}_2(t)\}\right|$ of the 3*R*-robot during 300 cycles, vs r and frequency ratio ω/ω_0, for $\rho = 0.7$, $\omega_0 = 7.0$ rad sec^{-1}.

For example, selecting in Fig. 5 several distinct cases, namely for r = 0.08, r = 0.30, r = 0.53, r = 1.10, r = 1.30 and r = 2.00, we have the different signal Fourier spectra clearly visible in Fig. 6.
For joints velocities 1 and 3 the results are similar to the verified ones for joint velocity 2.

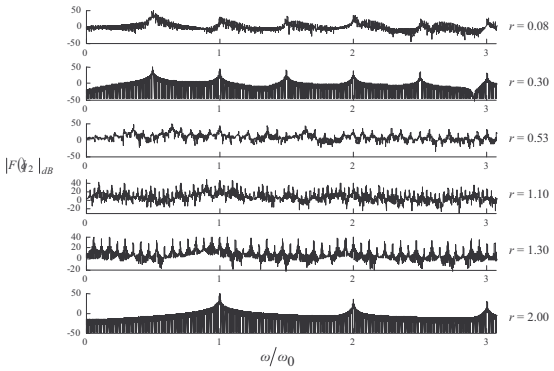

Fig. 6: $\left|F\{\dot{q}_2(t)\}\right|$ of the 3*R*-robot during 300 cycles, vs the frequency ratio ω/ω_0, for r = {0.08, 0.30, 0.53, 1.10, 1.30, 2.00}, $\rho = 0.7$, $\omega_0 = 7.0$ rad sec^{-1}.

In order to capture the time evolution of the joint variables we develop a second set of experiments.

One way of obtaining the time-dependent frequency content of a signal is to take the Fourier transform of a function over an interval around an instant τ, where τ is a variable parameter (Mallat, 1999). This mathematical tool is called the short-time or windowed Fourier transform (*WFT*) and may be defined as follows:

$$\left\{F_g f\right\}(\omega,\tau) = \int_{-\infty}^{+\infty} f(t)\,\overline{g(t-\tau)}\,e^{-it\omega}\,dt \qquad (8)$$

where $g(t)$ is the window function and $\tau, \omega \in \Re$. The multiplication by $g(t-\tau)$ localizes the Fourier integral in the neighborhood of $t = \tau$.
The slice of information provided by $\left\{F_g f\right\}(\omega,\tau)$ is represented in a time-frequency plane (t,ω) by a region whose location and width depends on the time-frequency spread of $g_{\omega,\tau}(t) = e^{it\omega} g(t-\tau)$. If $\mu(g)$ and $\sigma(g)$ are the centre and the radius, respectively, of the window function $g(t)$, then $\left\{F_g f\right\}(\omega,\tau)$ gives information about f and F, essentially in the region $I_t \times I_\omega$ of the time-frequency plane where $\hat{g} = F(g)$, $I_t \equiv [\mu(g) + \tau - \sigma(g), \mu(g) + \tau + \sigma(g)]$ and $I_\omega \equiv [\mu(\hat{g}) + \omega - \sigma(\hat{g}), \mu(\hat{g}) + \omega + \sigma(\hat{g})]$.

The Heisenberg uncertainty proves that the area of this region is:

$$\sigma(t)\,\sigma(\omega) \geq 1/2 \qquad (9)$$

and this principle states that precise localizations both, on time and frequency, are mutually exclusive. Thus this trade-off between temporal and frequency resolution always exist (Ozaktas, *et al.*, 2001). Moreover, the size of this region is independent of (t,ω), which means that the *WFT* has the same resolution across the time-frequency plane.

In the experiments we adopt two window functions, $\Psi := \{R_w, G_w\}$, namely rectangle and Gaussian windows $R_w(t) = 1$, and $G_w(t) = e^{-at^2/2}$, $(a = 18), t \in W_\Psi$. Moreover, we choose two that leads to non-overlapping time windows. In the sequel the corresponding *WFT*s are represented by F_{R_w} and F_{G_w}, respectively.

Figures 7-12 show $|F_\Psi\{\dot{q}_2(t)\}|$, with window width $W_\Psi = \{5, 50\}$ cycles, $\Psi := \{R_w, G_w$, for $\rho = 0.5$, $r = \{0.6, 1.289, 2.0\}$.

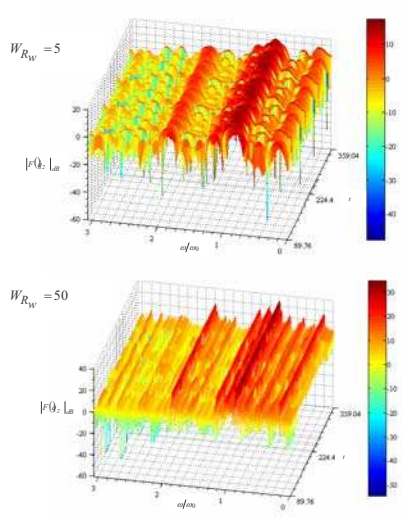

Fig. 7: $|F_{R_w}\{\dot{q}_2(t)\}|$ of the 3*R*-robot during 300 cycles, vs time and frequency ratio ω/ω_0, for $\rho = 0.5$, $r = 0.6$, $\omega_0 = 7.0$ rad sec^{-1} and $W_{R_w} = \{5, 50$ cycles.

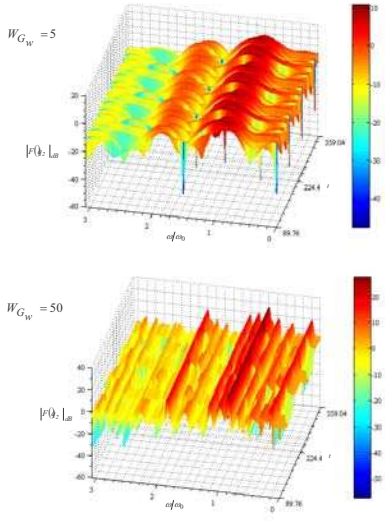

Fig. 8: $|F_{G_w}\{\dot{q}_2(t)\}|$ of the 3*R*-robot during 300 cycles, vs time and frequency ratio ω/ω_0, for $\rho = 0.5$, $r = 0.6$, $\omega_0 = 7.0$ rad sec^{-1} and $W_{G_w} = \{5, 50\}$ cycles.

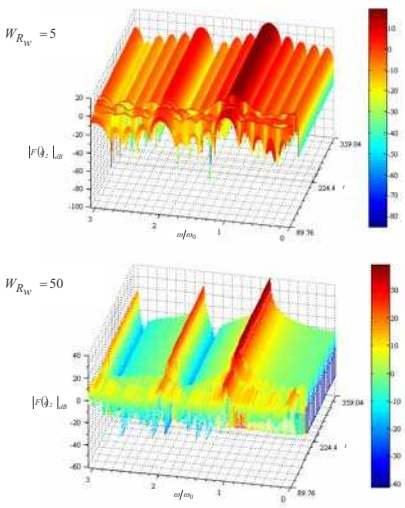

Fig. 9: $|F_{R_w}\{\dot{q}_2(t)\}|$ of the 3*R*-robot during 300 cycles, vs time and frequency ratio ω/ω_0, for $\rho = 0.5$, $r = 1.289$, $\omega_0 = 7.0$ rad sec^{-1} and $W_{R_w} = \{5, 50$ cycles.

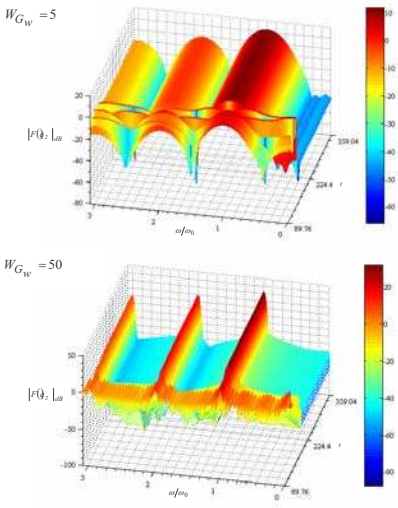

Fig. 10: $|F_{G_w}\{\dot{q}_2(t)\}|$ of the 3*R*-robot during 300 cycles, vs time and frequency ratio ω/ω_0, for $\rho = 0.5$, $r = 1.289$, $\omega_0 = 7.0$ rad sec^{-1} and $W_{G_w} = \{5, 50\}$ cycles.

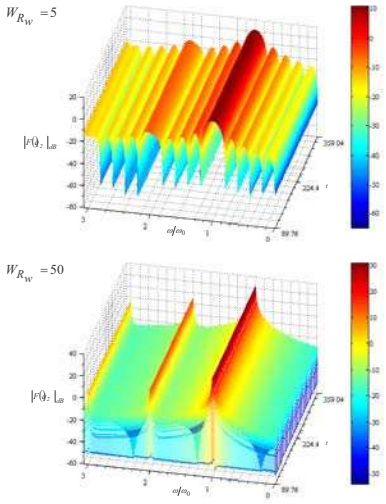

Fig. 11: $\left|F_{R_W}\{\dot{q}_2()\}\right|$ of the 3*R*-robot during 300 cycles, vs time and frequency ratio ω/ω_0, for $\rho = 0.5$, r = 2.0, ω_0 = 7.0 rad $\sec^{-1}$ and $W_{R_W} = \{5, 50$ cycles.

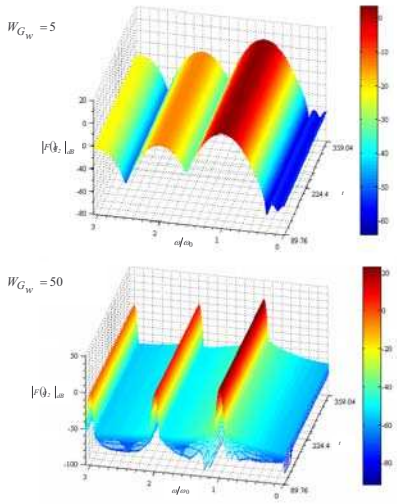

Fig. 12: $\left|F_{G_W}\{\dot{q}_2()\}\right|$ of the 3*R*-robot during 300 cycles, vs time and frequency ratio ω/ω_0, for $\rho = 0.5$, r = 2.0, ω_0 = 7.0 rad $\sec^{-1}$ and $W_{G_W} = \{5, 50\}$ cycles.

We verify that choosing a shorter (larger) time window W_Ψ increases (decreases) the temporal resolution but, on the other hand, decreases (increases) the frequency resolution.

In Fig. 7-8 (r = 0.6) we observe that the distribution of the signal energy dependents on the time evolution.

In fact, the signal energy of the fundamental harmonic oscillates periodically and we verify that a large amount of the signal energy concentrates at several *foh*.

In Fig. 9-10 (r = 1.289) we verify that we have two distinct regions: a first one for the leading 60 cycles and a second for the remaining 240 cycles. In the first region we have a signal energy distribution along all frequencies, while in the second the energy is concentrated in the fundamental and multiple higher harmonics.

Finally, in Fig. 11-12 (r = 2.0) we get a regular behavior and the *WFT*s are invariant with time.

In all figures 7-12, the phenomena occur independently of the shape $\Psi := \{R_W, G_W$ or the width W_Ψ of the time window.

5. CONCLUSIONS

This paper discussed several aspects of the phenomena generated by the pseudoinverse-based trajectory control of the 3*R* redundant manipulators.

The closed-loop pseudoinverse's method leads to non-optimal responses, both for the manipulability and the repeatability. Bearing these facts in mind the chaotic responses were analyzed from different point of views, namely phase plane and Fourier Transform.

The results revealed the appearance of radial distances for which a large part of the energy is distributed in *fractional order harmonics.* In order to capture the time evolution of the joint variables we develop a set of experiments based on the *WFT*. The results showed that the frequencies of the joint velocity depend on the time evolution.

REFERENCES

Klein, C. A. and C. C Huang (1983). Review of Pseudoinverse Control for Use With Kinematically Redundant Manipulators. *IEEE Trans. Syst. Man, Cyber*, **vol. 13**, pp. 245-250.

Nakamura, Y. (1991). *Advanced Robotics: Redundancy and Optimization*. Addinson-Wesley.

Doty, K.L., C. Melchiorri and C. Bonivento (1993). A Theory of Generalized Inverses Applied to Robotics. *International Journal of Robotics Research*, **vol. 12**, pp. 1-19.

Siciliano, B. (1990). Kinematic Control of Redundant Robot Manipulators: A Tutorial. *Journal of Intelligent and Robotic Systems*, **vol. 3**, pp. 201-212.

Duarte, F. and J. A. T. Machado (2002). Chaotic Phenomena and Fractional-Order Dynamics in the Trajectory Control of Redundant Manipulators. In: *Nonlinear Dynamics*, **vol. 29**, n. 1-4, pp. 315-342. Kluwer, USA.

Yoshikawa, T. (1988). *Foundations of Robotics: Analysis and Control*. MIT Press.

Mallat, S. (1999). *A Wavelet Tour of Signal Processing*. Academic Press.

Ozaktas, H. M., Z. Zalevsky and M. A. Kutay (2001). *The Fractional Fourier Transform with Applications in Optics and Signal Processing*. John Wiley & Sons Ltd.